

Supporting Information

Self-catalysed folding of single chain nanoparticles (SCNPs) by NHC-mediated intramolecular benzoin condensation

Sofiem Garmendia,^{a,b,c,d} Andrew P. Dove,^d Daniel Taton^{a,b} and Rachel K. O'Reilly^{*d}

^a *Laboratoire de Chimie des Polymères Organiques (LCPO), Université de Bordeaux, IPB-ENSCBP, F-33607 Pessac Cedex, France*

^b *Laboratoire de Chimie des Polymères Organiques (LCPO), Centre National de la Recherche Scientifique, 16 Avenue Pey Berland, F-33607 Pessac Cedex, France*

^c *Department of Chemistry, University of Warwick, Coventry, CV4 7AL, UK*

^d *School of Chemistry, The University of Birmingham, Edgbaston, Birmingham, B15 2TT, UK*

Table of contents

Experimental

Synthesis of monomer 1	S3
Synthesis of linear precursor 2	S3–S4
Synthesis of linear precursor 3	S4–S5
Synthesis of linear coPIL 4	S5–S6
Synthesis of SCNP 5	S6–S10
Synthesis of SCNP 6	S10–S11
Synthesis of linear polymer model 7	S12
Synthesis of molecular model 8	S13
Transesterification reaction	S13–S19

References	S19
-------------------	------------

Experimental

Synthesis of monomer 1: Synthesis of 4-vinylbenzylethylbenzimidazolium chloride ([ViEBIm]Cl)

N-Ethylbenzimidazole was synthesised according to the previously reported¹⁻³ procedure from Taton, O'Reilly *et al.* Benzimidazole (5 g, 42.32 mmol, 1 eq.) was first dissolved in DMF (20 mL), potassium hydroxide was then added (4.75 g, 106 mmol, 2.5 eq.). The solution was stirred for 30 minutes before the drop-wise addition of ethyl bromide (3.45 mL, 46.55 mmol). After stirring at room temperature for 24 h, the reaction mixture was diluted using H₂O (50 mL), the aqueous phase was then extracted with dichloromethane (4 x 25 mL). The organic phases were combined, dried over MgSO₄ and evaporated, yielding *N*-ethylbenzimidazole as a viscous yellow oil (4.93 g, 33.8 mmol, 80% yield) ¹H NMR (DMSO-*d*₆): δ = 8.25 (s, 1H, N-CH-N), 7.69-7.20 (m, 4H, aromatics), 4.12 (t, 2H, N-CH₂-CH₃), 1.32 (t, 3H, -CH₃).

A portion of *N*-ethylbenzimidazole (4.65 mL, 31.8 mmol, 1 eq.) was then dissolved in acetonitrile (20 mL) within a Schlenk tube, this was immediately followed by the addition of 4-vinylbenzylchloride (4.82 g, 31.8 mmol, 1 eq.) After stirring for 24 h at 80 °C, the crude reaction mixture was precipitated into ethyl acetate (20 mL) and dried under vacuum to remove the solvent, yielding the target monomer 4-vinylbenzylethylbenzimidazolium chloride as a white powder (8.64 g, 28.9 mmol, yield = 91%). ¹H NMR (DMSO-*d*₆): δ = 9.7 (s, 1H, N-CH-N), 8.12-7.1 (m, 8H, aromatics), 6.7 (dd, 1H, Ph-CH-CH₂), 5.9 (s, 2H, Ph-CH₂-N), 5.8 (d, 1H, CH=CH₂), 5.2 (d, 1H, CH=CH₂), 4.2 (dd, 2H, N-CH₂-CH₃), 1.3 (t, 3H, -CH₂-CH₃). Characterisation matches that previously reported in the literature.¹⁻³

Synthesis of linear precursor 2

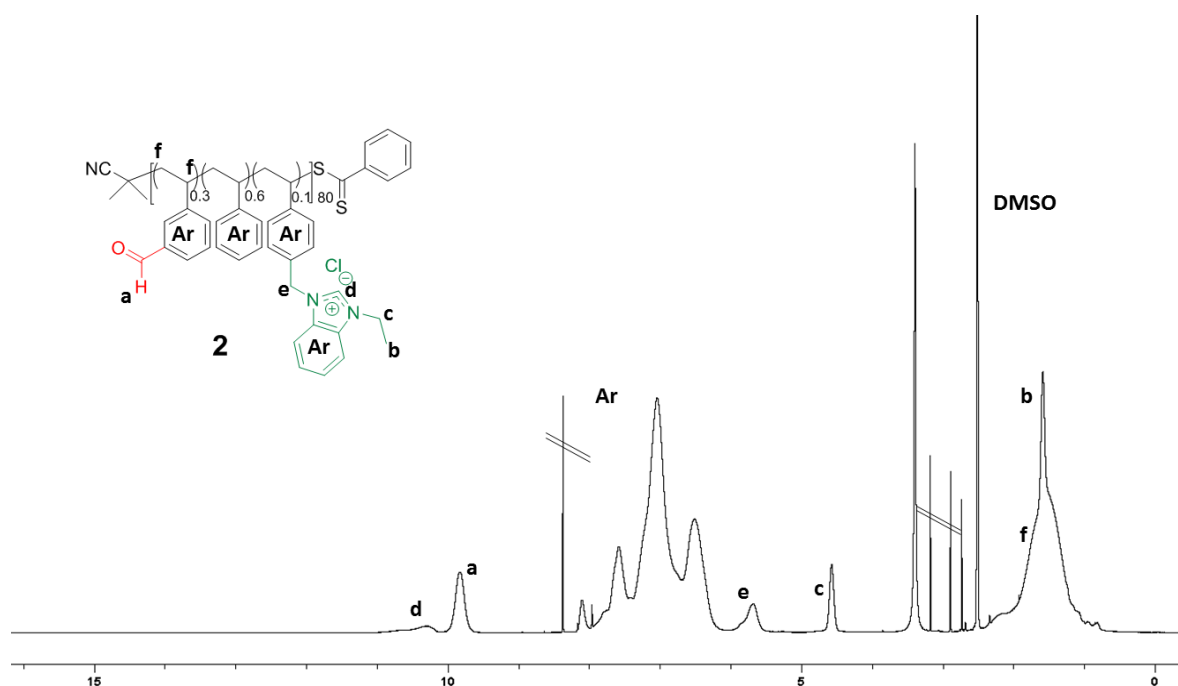


Figure S1. ¹H NMR spectrum of copolymer 2 in DMSO-*d*₆.

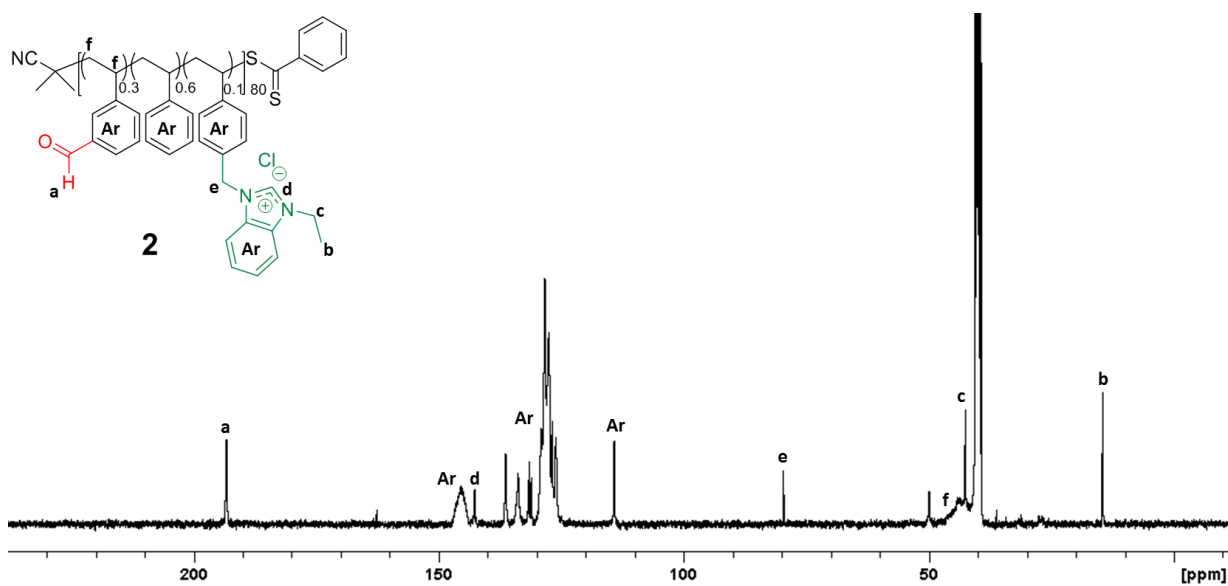


Figure S2. ^{13}C NMR spectrum of copolymer **2** in $\text{DMSO-}d_6$.

Synthesis of linear precursor **3**

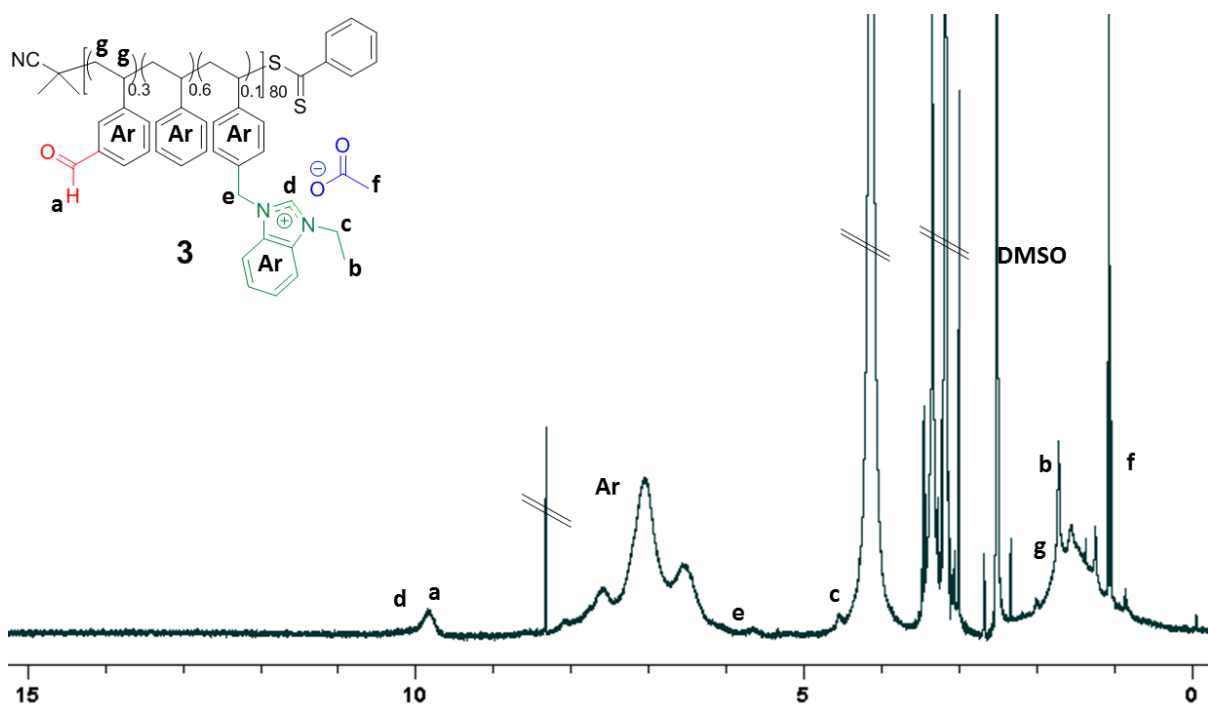


Figure S3. ^1H NMR spectrum of copolymer **3** in $\text{DMSO-}d_6$

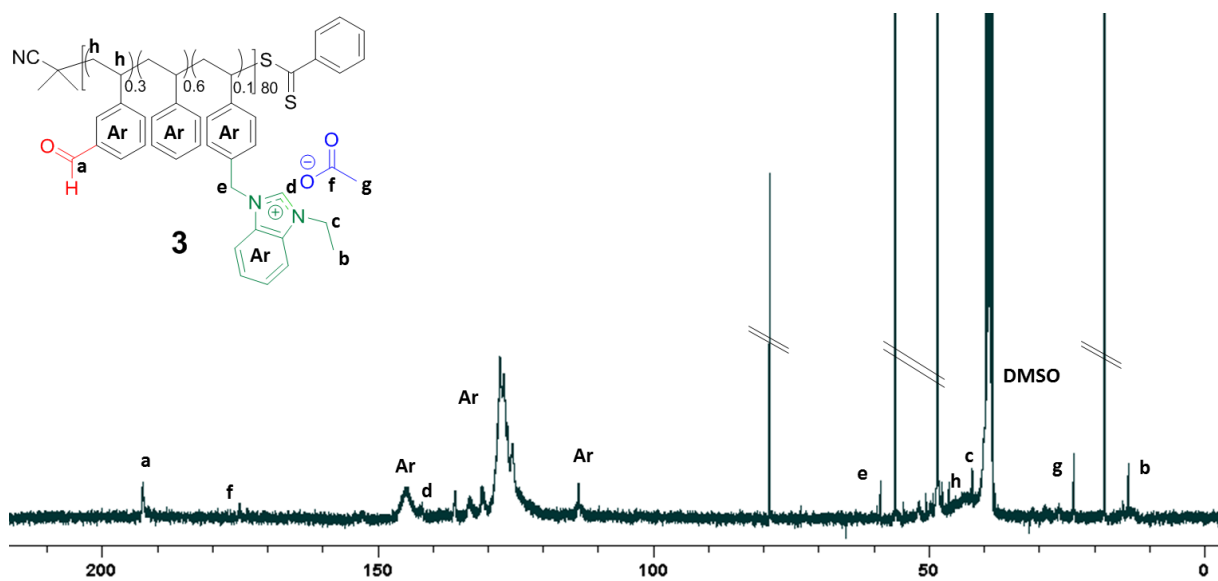


Figure S4. ^{13}C NMR spectrum of copolymer **3** in $\text{DMSO-}d_6$.

Synthesis of linear coPIL **4**

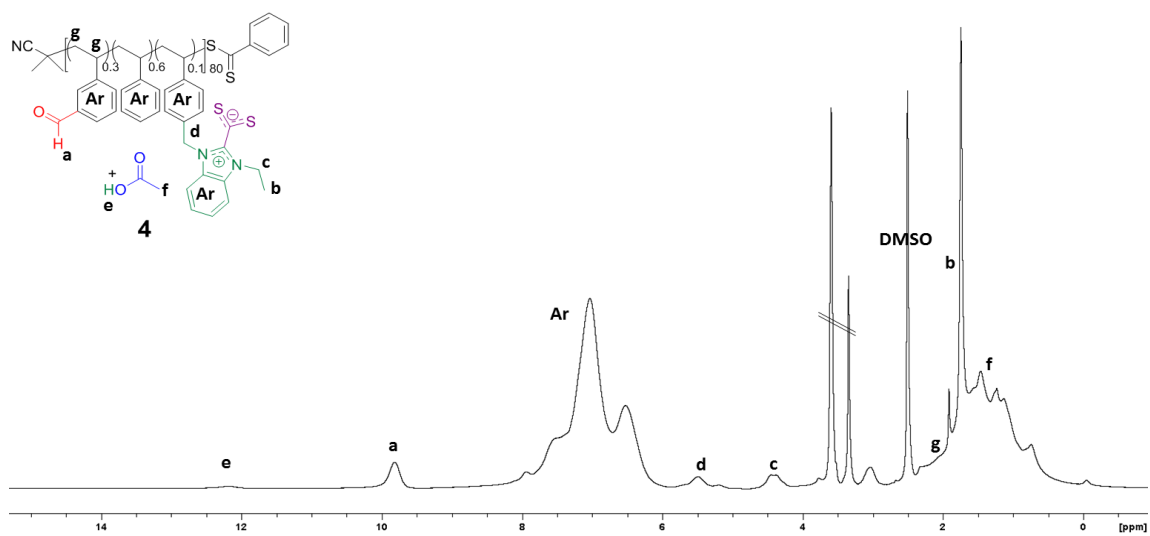


Figure S5. ^1H NMR spectrum of copolymer **4** in $\text{DMSO-}d_6$.

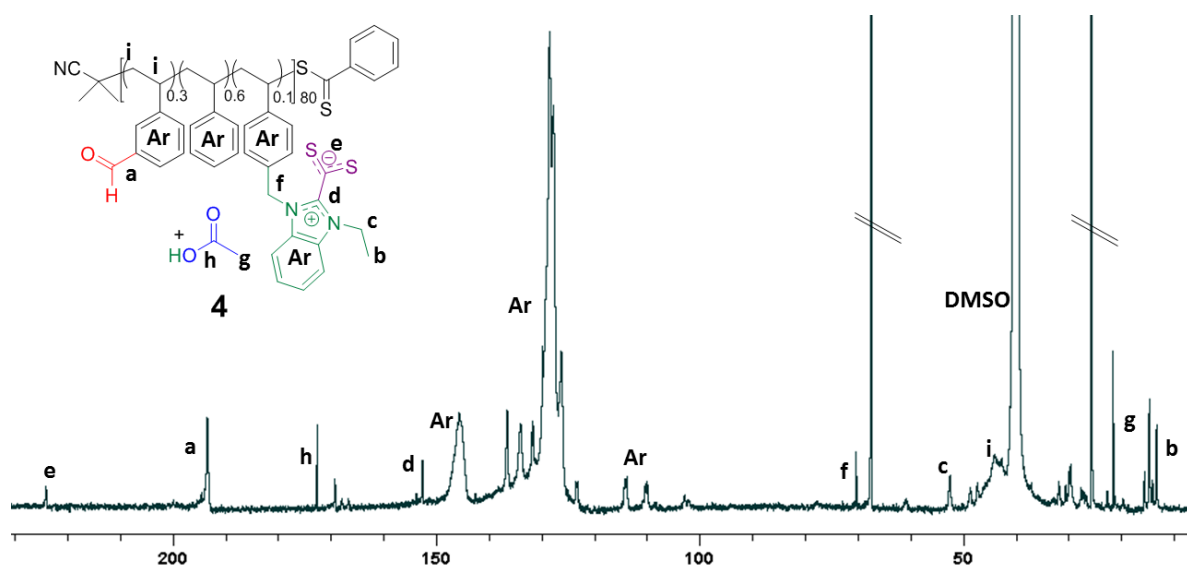


Figure S6. ^{13}C NMR spectrum of copolymer **4** in $\text{DMSO-}d_6$.

Synthesis of SCNP **5**.

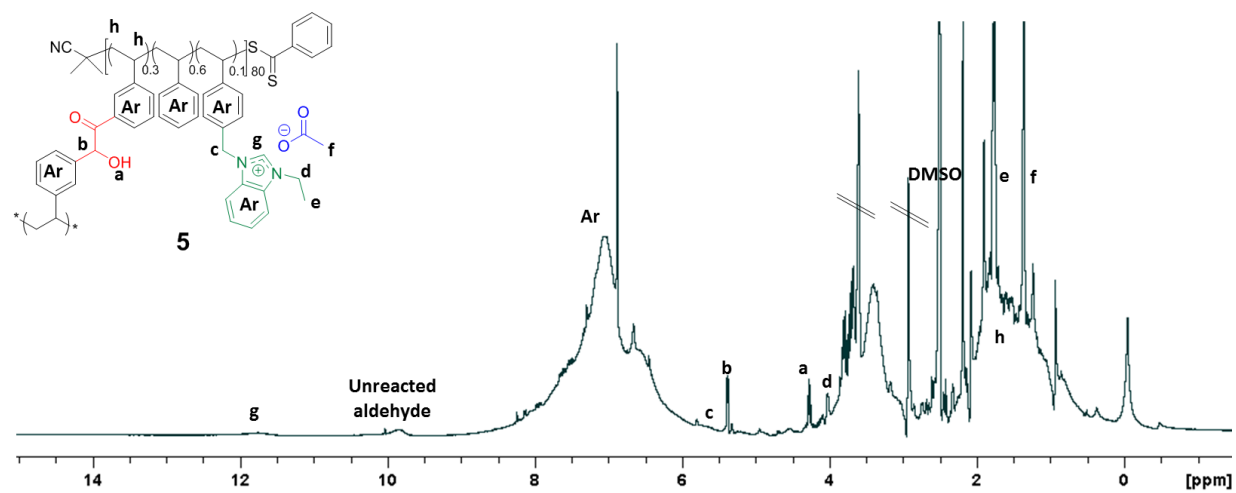


Figure S7. ^1H NMR spectrum of SCNP **5** in $\text{DMSO-}d_6$.

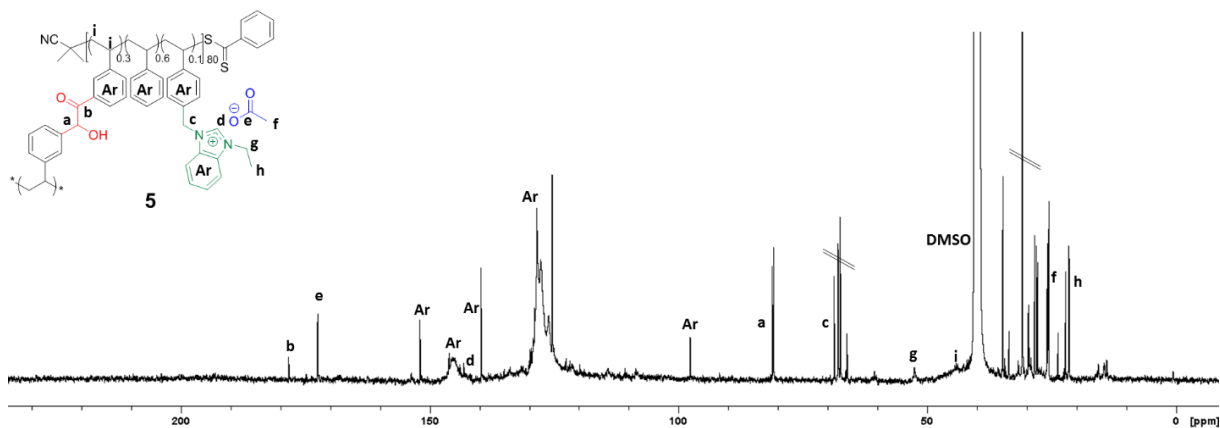


Figure S8. ^{13}C NMR spectrum of copPIL **5** in $\text{DMSO-}d_6$.

The multiplicity-edited HSQC NMR spectrum was used to confirm the incorporation of the benzoin moiety into SCNP **5**, with a clear coupling observed between the signal at ~ 5.4 ppm and the tertiary carbon corresponding to the $-\text{CH}-$ of the benzoin bridge.

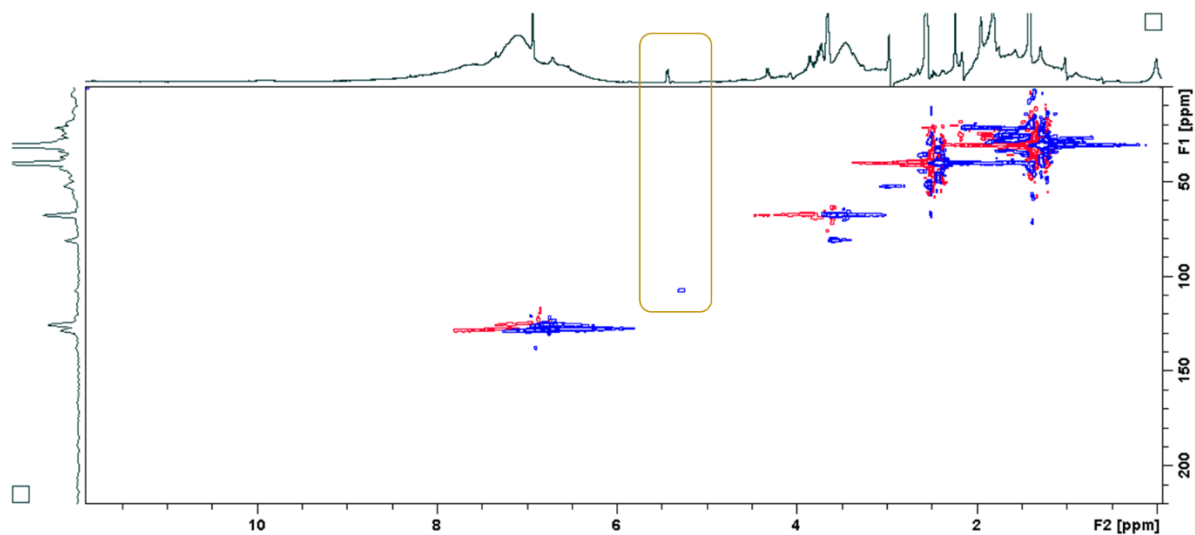


Figure S9. Representative multiplicity-edited HSQC spectrum of SCNP **5** in $\text{DMSO-}d_6$, with tertiary and primary carbons identified in blue, and quaternary and secondary carbons identified in red.

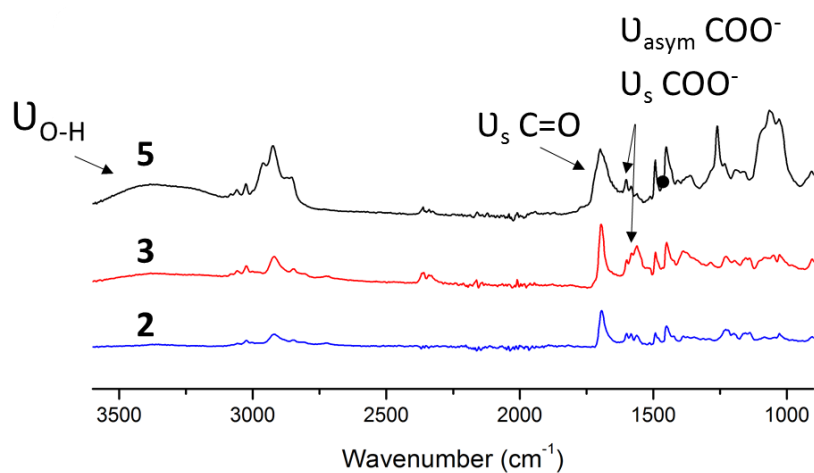


Figure S10. Representative FTIR spectrum of SCNP 5 (in black), linear polymer 3 (in red) and linear polymer 2 (in blue).

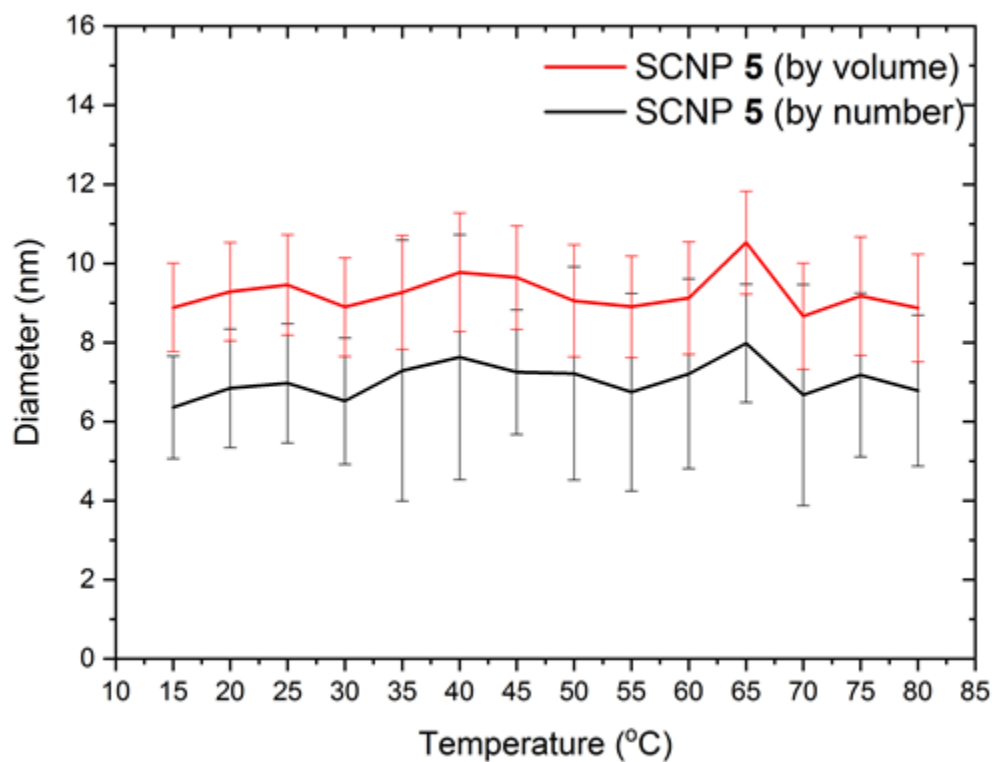


Figure S11. Hydrodynamic diameter-temperature correlation obtained for SCNP 5 by variable temperature dynamic light scattering (DLS) in THF (Conc.: 1 mg mL⁻¹; 173° back-scattering detector; average value of 4 runs is reported along with the error corresponding to the standard deviation in the measurements; solid red line corresponds to values obtained for the volume distribution, whilst the solid black refers to the number distribution).

Diffusion Ordered Spectroscopy (DOSY). The folded SCNP and the linear copolymer were distinguished according to their diffusion coefficients as determined by DOSY NMR spectroscopy, which correlates their hydrodynamic radius to their relative rates of diffusion through DMSO-*d*₆. Full details for the experimental conditions used for DOSY NMR spectroscopy can be found within the experimental of the main article. Calculation of the hydrodynamic radius and therefore the diameter was done so by applying the Stokes-Einstein equation.^{4,5}

Stokes-Einstein equation:

$$D = \frac{kT}{6\pi\eta r}$$

$$k = 1.38 \cdot 10^{-23} \text{ J K}^{-1}$$

$$D = 3.14 \cdot 10^{-11} \text{ m}^2 \text{ s}^{-1}$$

$$T = 298 \text{ K}$$

$$\eta \text{ DMSO viscosity} = 1.99 \cdot 10^{-3} \text{ Pa s}$$

$$R \text{ (polymer } \mathbf{5}) = 1.15 \text{ nm}; D = 2.3 \text{ nm}$$

$$R \text{ (polymer } \mathbf{2}) = 3.3 \text{ nm}; D = 6.6 \text{ nm}$$

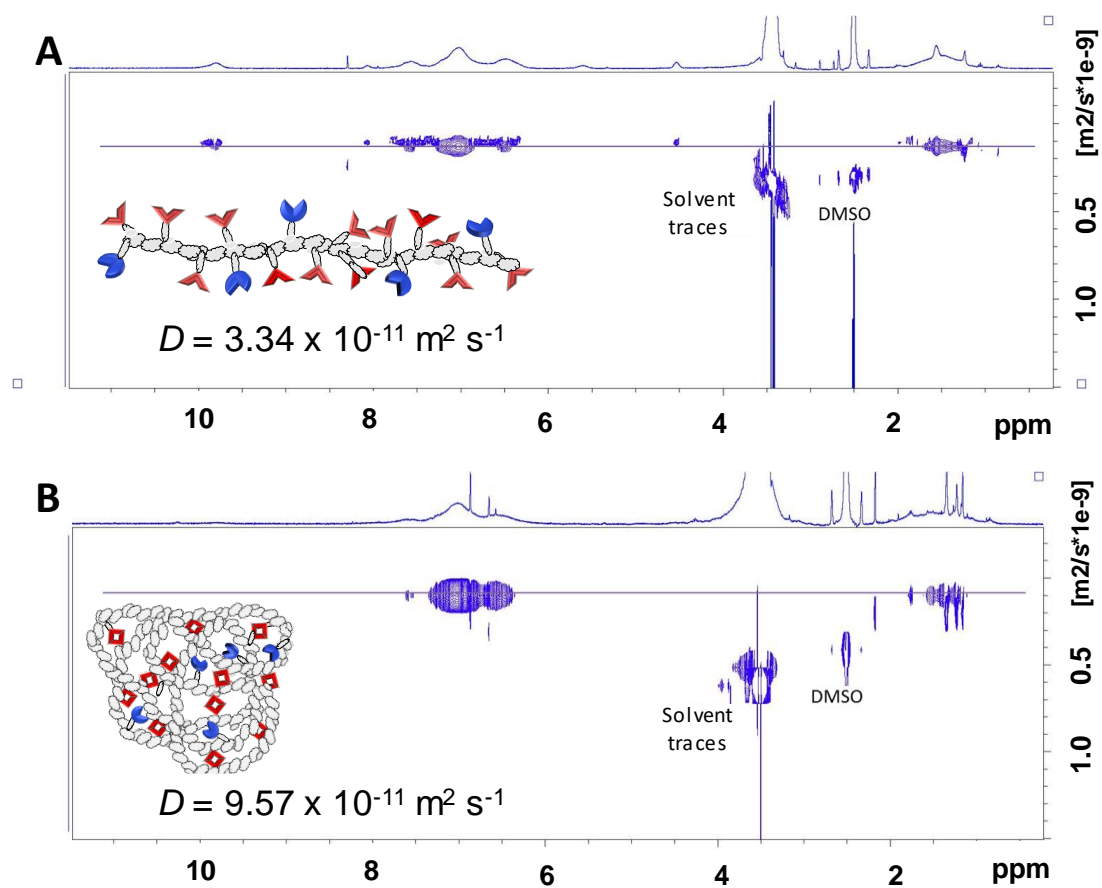


Figure S12. DOSY NMR spectroscopy in DMSO-*d*₆ for linear precursor **2** (A) and folded SCNP **5** (B).

Synthesis of SCNP **6**

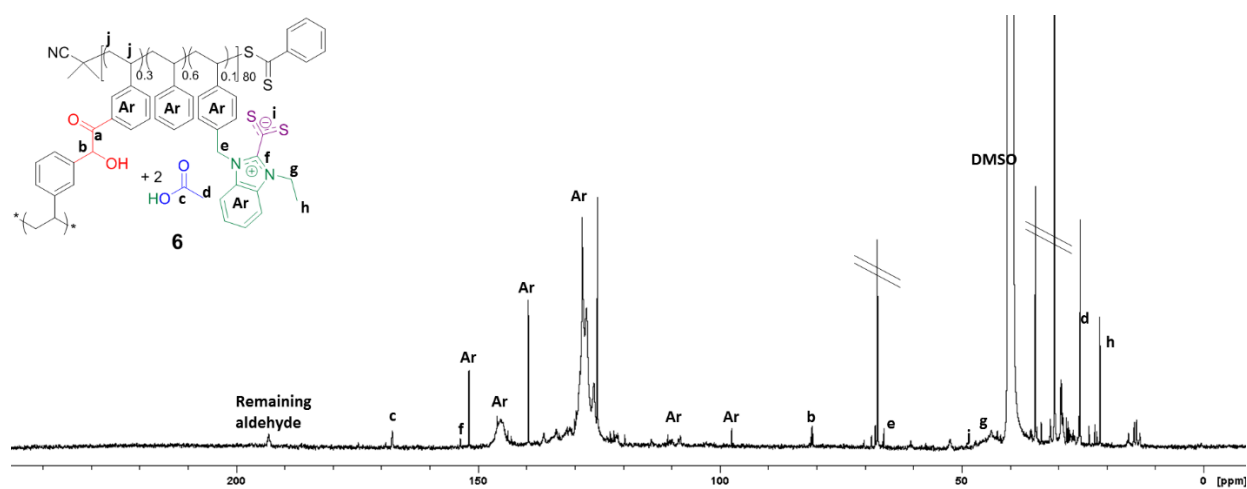


Figure S13. ¹³C NMR spectrum of SCNP **6** in DMSO-*d*₆.

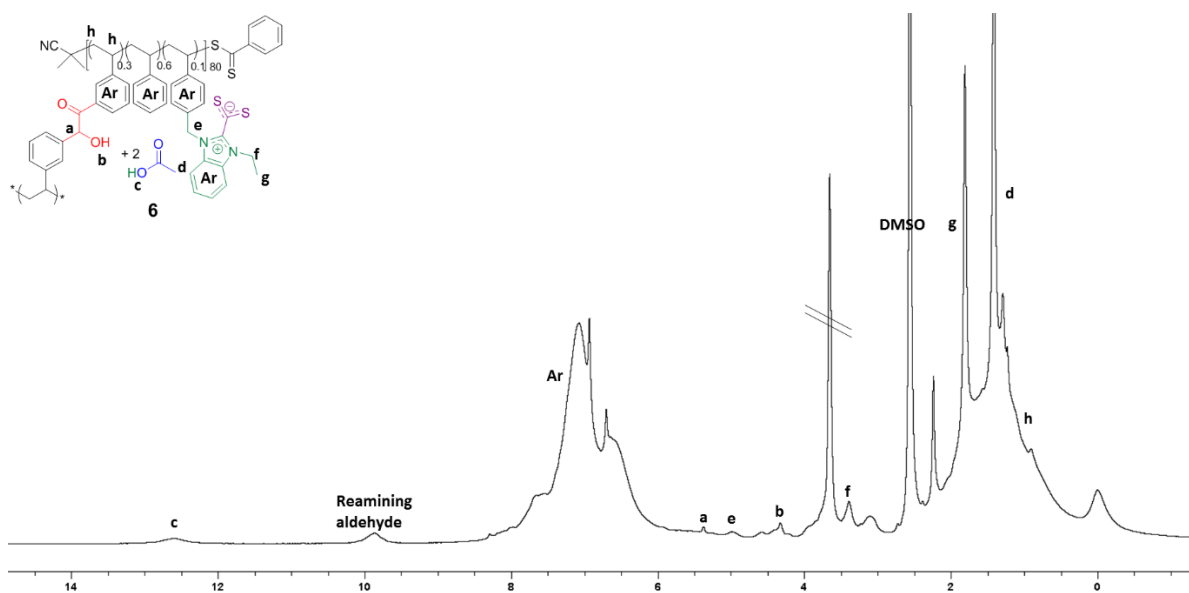


Figure S14. ^1H NMR spectrum of SCNP **6** in $\text{DMSO-}d_6$.

The insertion carbon disulfide into the NHC moiety was further evidenced by FTIR, as indicated by the appearance of the characteristic asymmetric CS_2^- vibration at $\sim 1030\text{ cm}^{-1}$, as seen in **Fig. S15**.^{6,7}

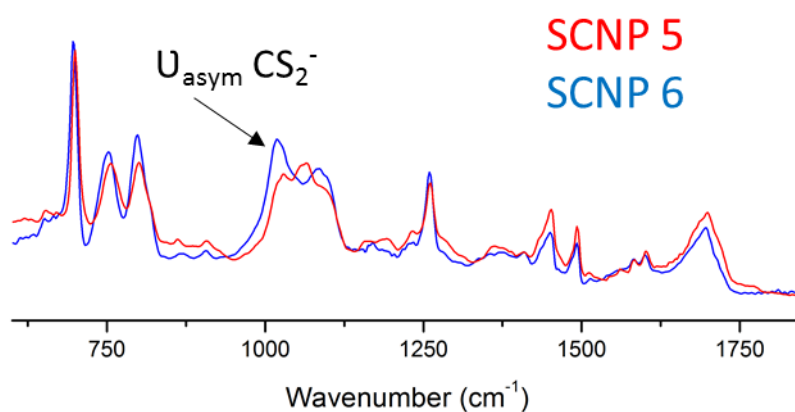


Figure S15. FTIR spectrum of SCNP **5** (in red) and NHC- CS_2^- functionalised SCNP **6** (in blue) showing the appearance of the characteristic vibrational signal of CS_2^- (at $\sim 1030\text{ cm}^{-1}$) when forming the betaine.

Synthesis of linear model polymer 7

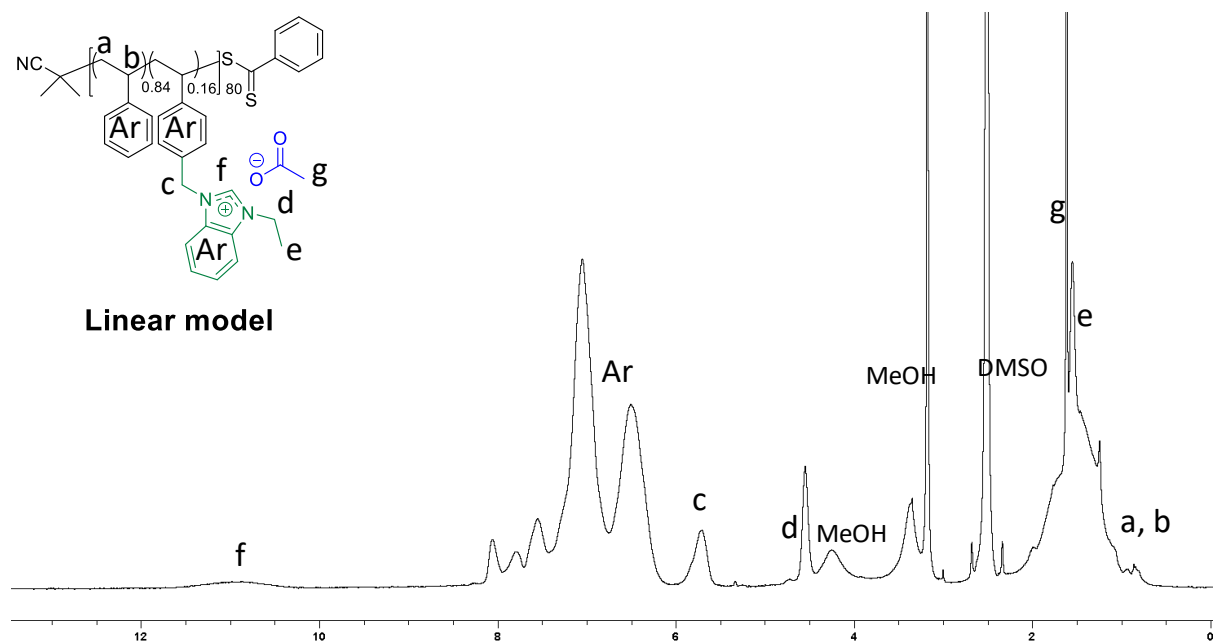


Figure S16. ¹H NMR spectrum of linear model 7 in DMSO-*d*₆.

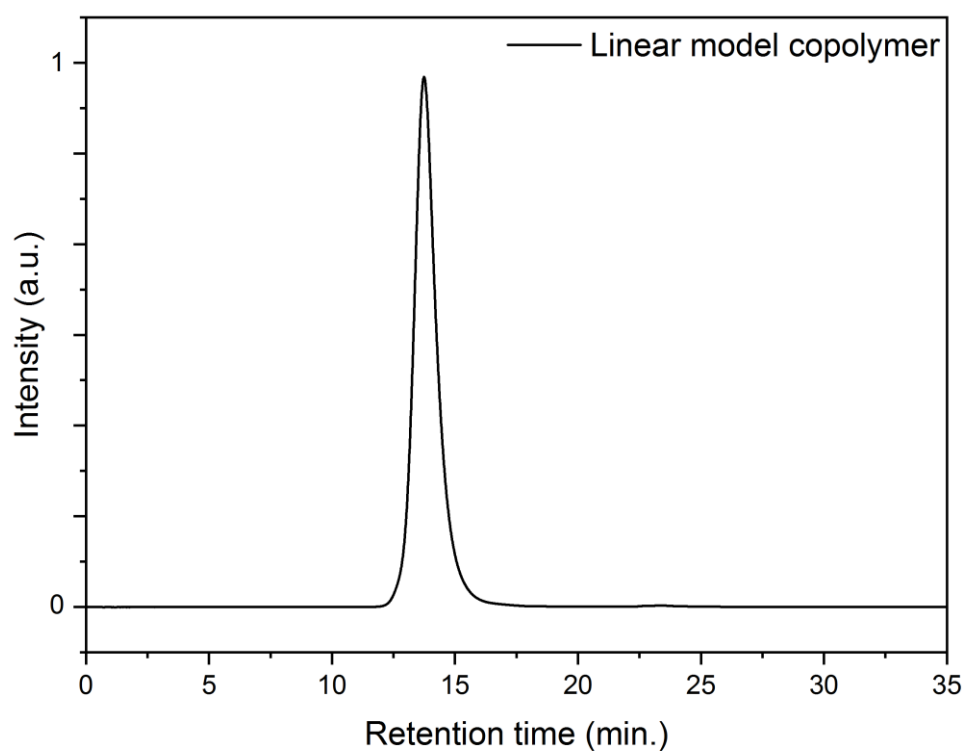


Figure S17. SEC trace corresponding to (bis(trifluoromethane)sulfonimide) TFSI-decorated linear model 7 in DMF (10 mM NH₄⁺BF₄⁻; UV detector; SEC analysis: $D_M = 1.1$; $M_n = 12.7$ kDa).

Synthesis of molecular model 8

Monomer **1** (0.25 g, 0.83 mmol, 1 eq.) was first solubilised in methanol (2 mL). Potassium acetate (0.1 g, 1 mmol, 1.2 eq.) was then added and the reaction carried out at room temperature with stirring for 16 h. The solution was then filtered to remove the KCl side-product and the filtrate dried under reduced pressure. Yield >95%. $^1\text{H NMR}$ ($\text{DMSO-}d_6$): $\delta = 10.9\text{--}10.1$ (br, 1H, $\text{N}=\text{CH-N}$), $9.9\text{--}9.6$ (br, 3H, H-CO-), $8.2\text{--}6.1$ (br, 53.1 H, Ar-), $5.9\text{--}5.5$ (br, 2H, $\text{Ar-CH}_2\text{-N}$), $4.7\text{--}4.5$ (br, 2H, $\text{N-CH}_2\text{-CH}_3$), $2.2\text{--}0.9$ (br, 30.2 H, backbone, $\text{CH}_2\text{-CH}_3$). Characterisation matches that reported in the literature.³

Transesterification reaction

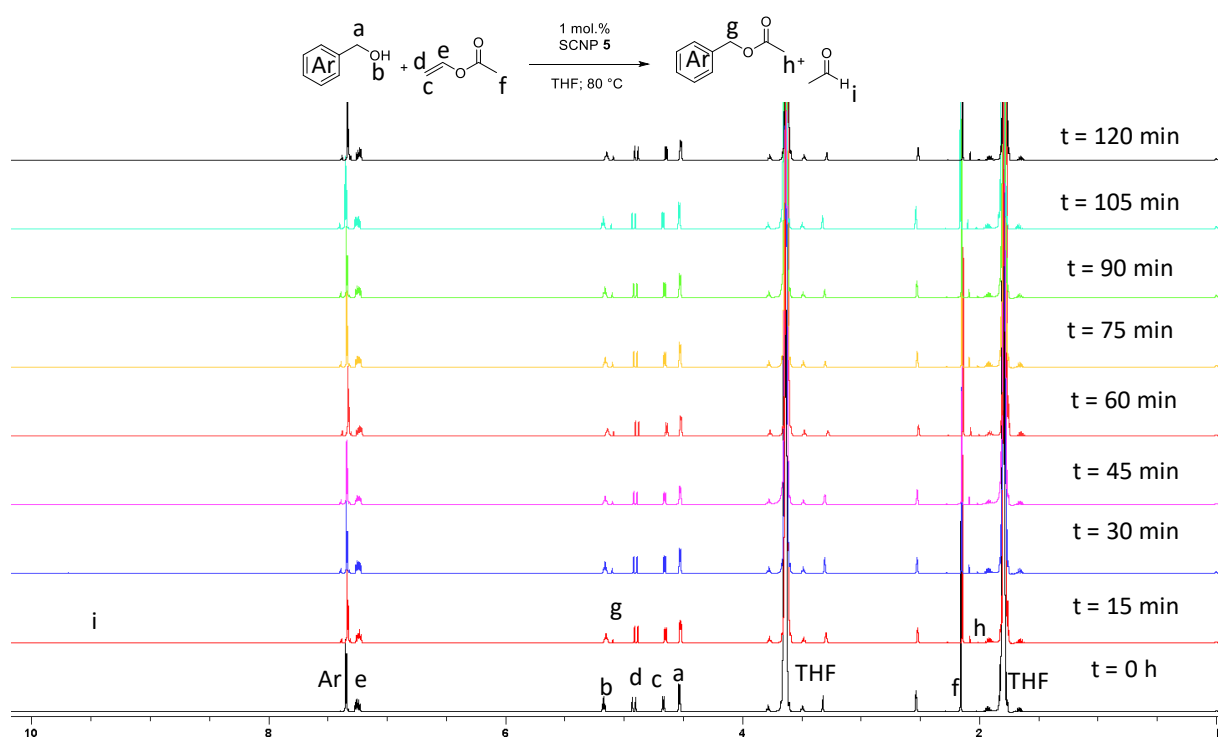


Figure S18. Reaction kinetics for run 1 (Table 1) monitored by $^1\text{H NMR}$ spectroscopy in $\text{DMSO-}d_6$.

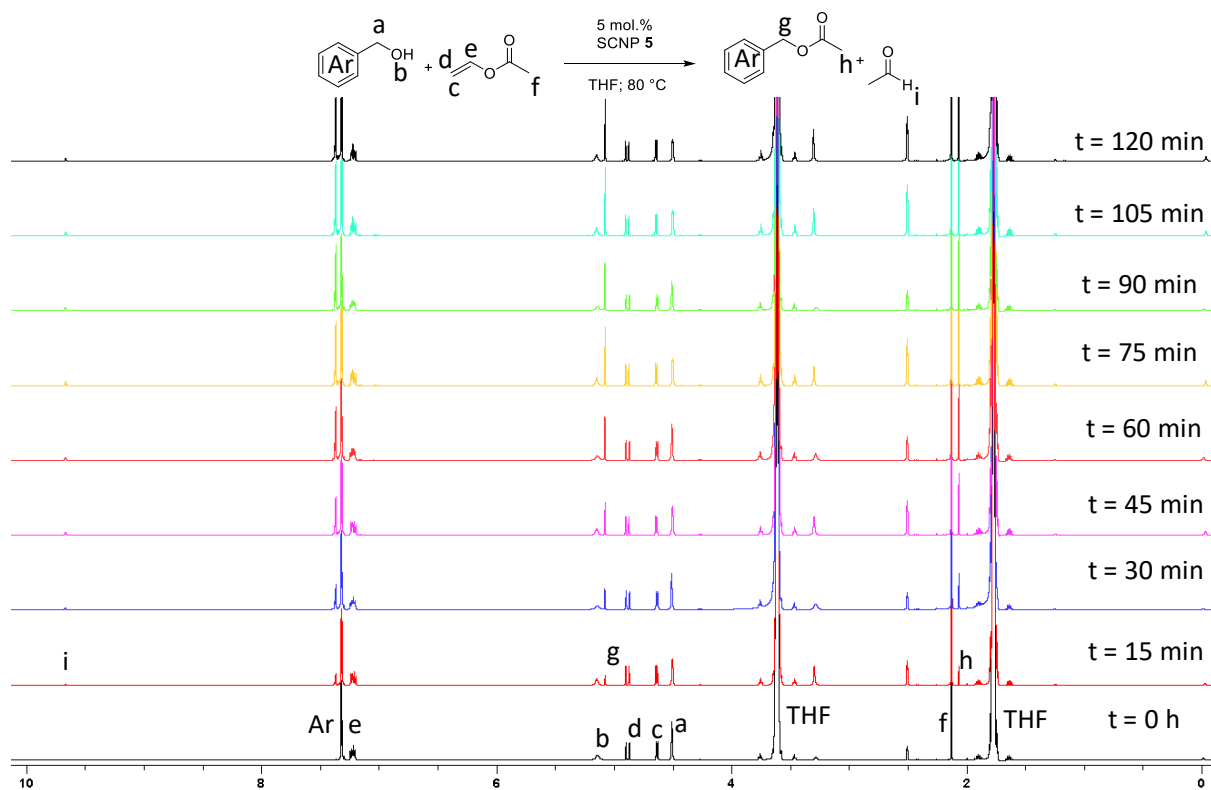


Figure S19. Reaction kinetics for run 2 (Table 1) monitored by ^1H NMR spectroscopy in DMSO- d_6 .

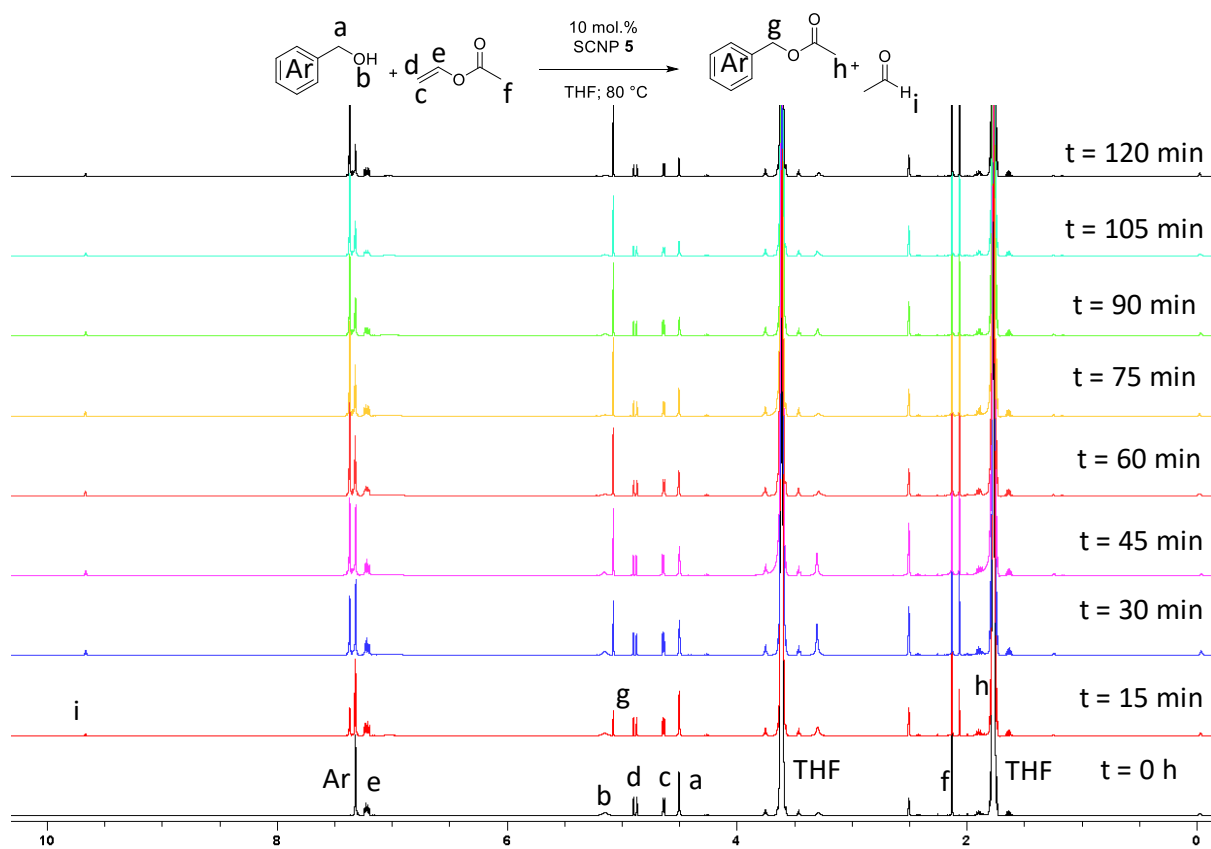


Figure S20. Reaction kinetics for run 3 (Table 1) monitored by ^1H NMR spectroscopy in DMSO- d_6 .

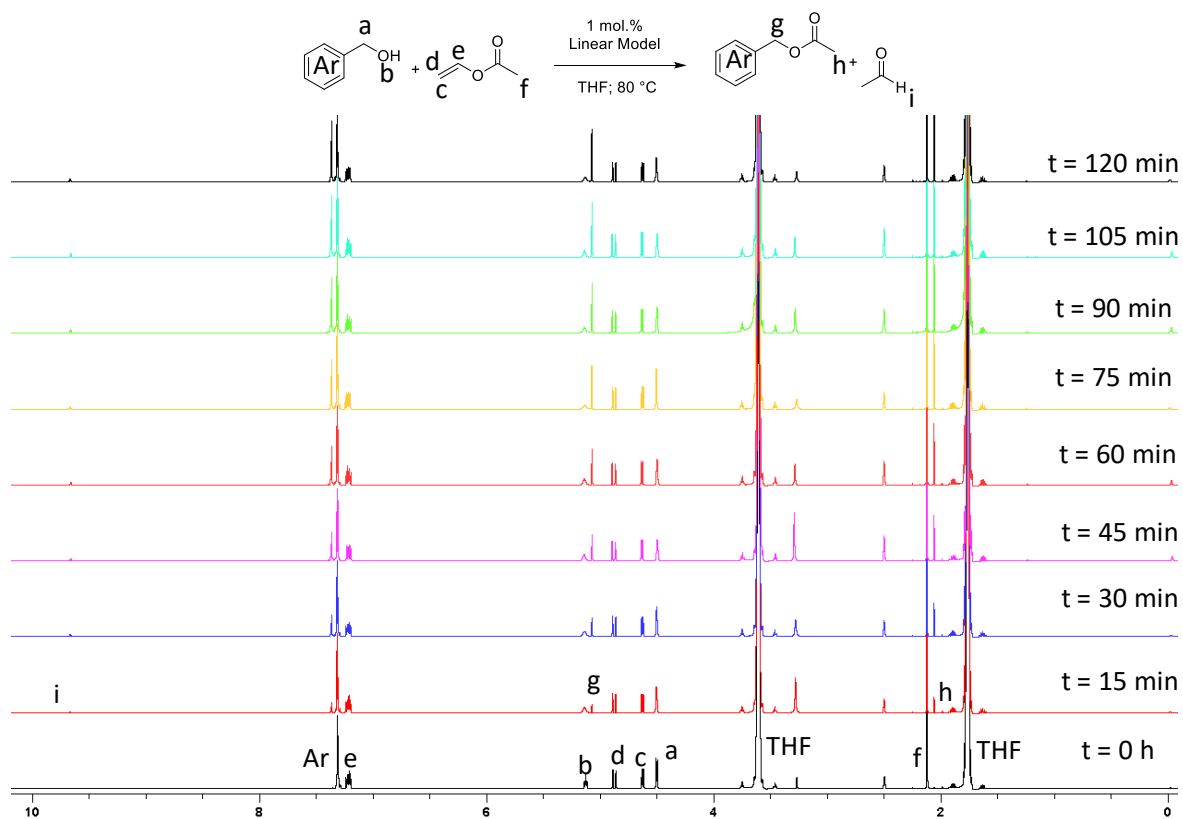


Figure S21. Reaction kinetics for run 4 (Table 1) monitored by ^1H NMR spectroscopy in $\text{DMSO-}d_6$.

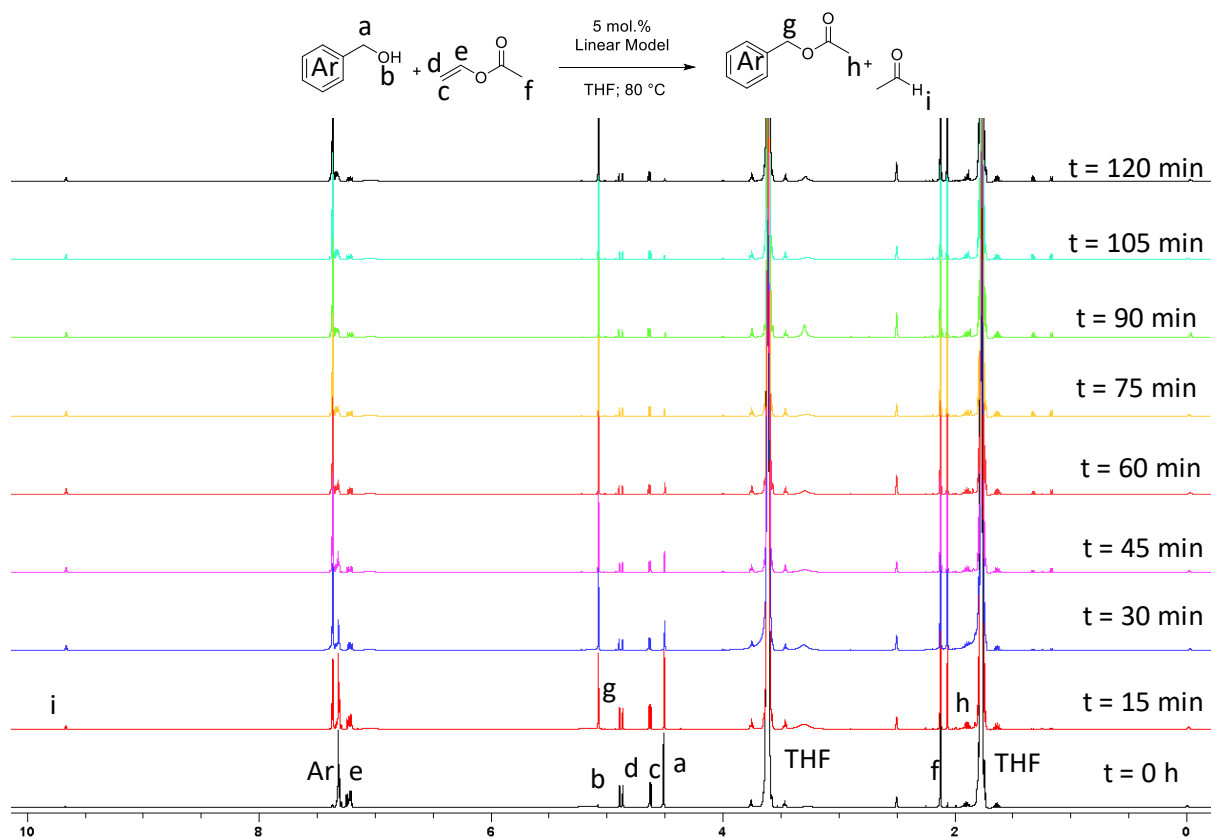


Figure S22. Reaction kinetics for run 5 (Table 1) monitored by ^1H NMR spectroscopy in $\text{DMSO-}d_6$.

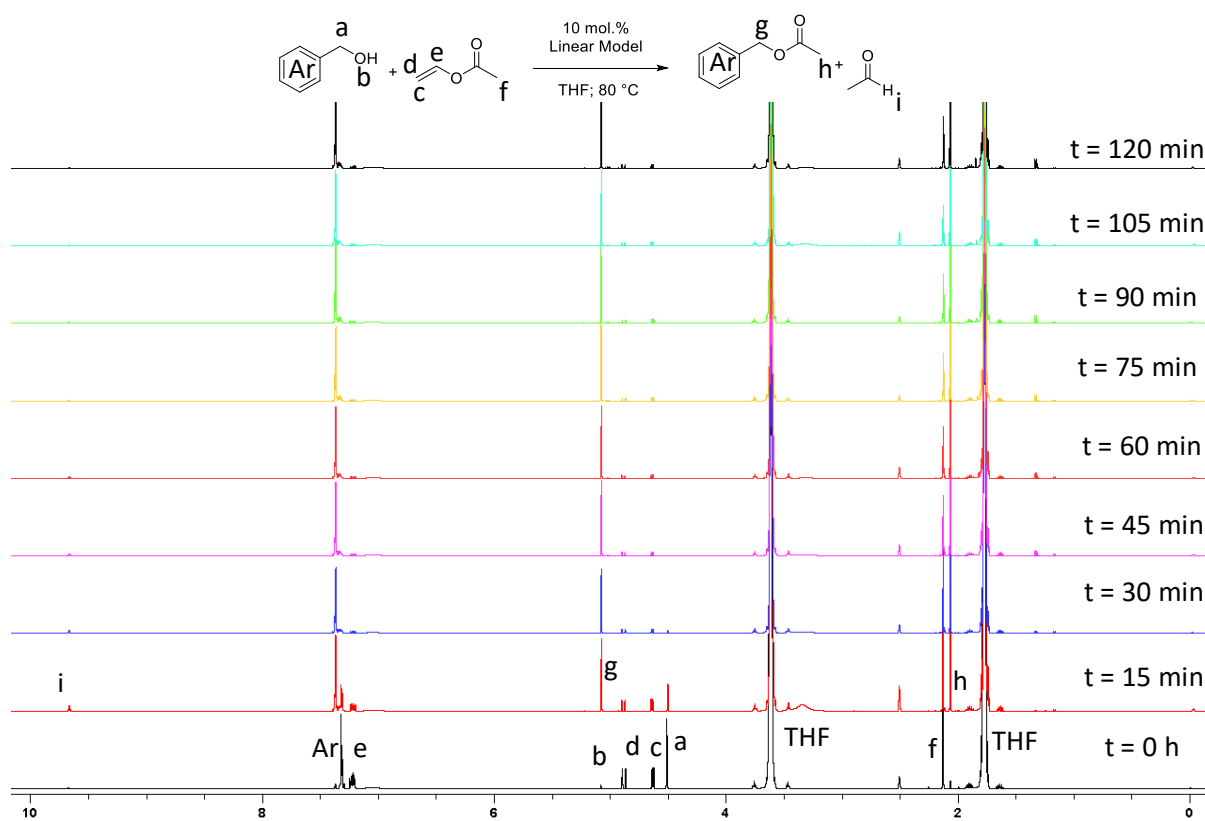


Figure S23. Reaction kinetics for run 6 (Table 1) monitored by ^1H NMR spectroscopy in $\text{DMSO-}d_6$.

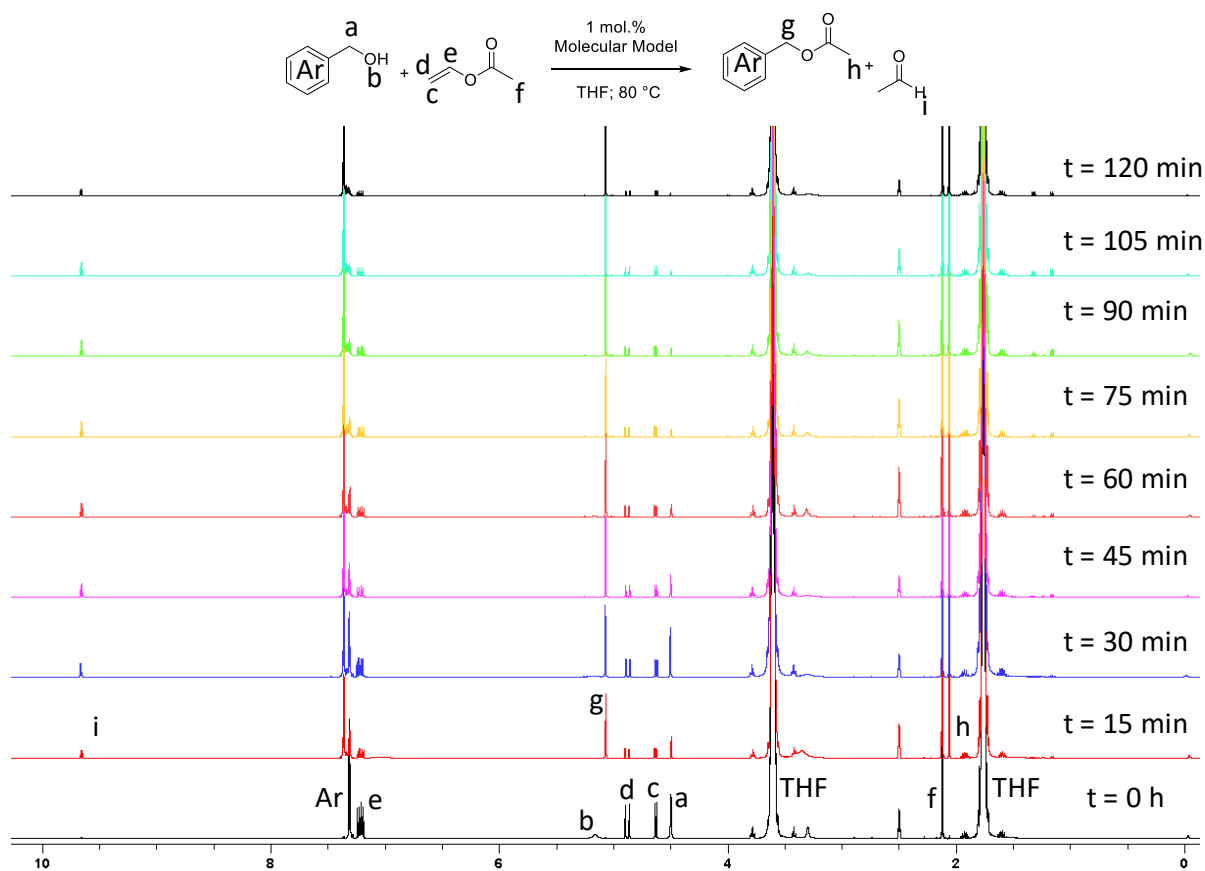


Figure S24. Reaction kinetics for run 7 (Table 1) monitored by ^1H NMR spectroscopy in $\text{DMSO-}d_6$.

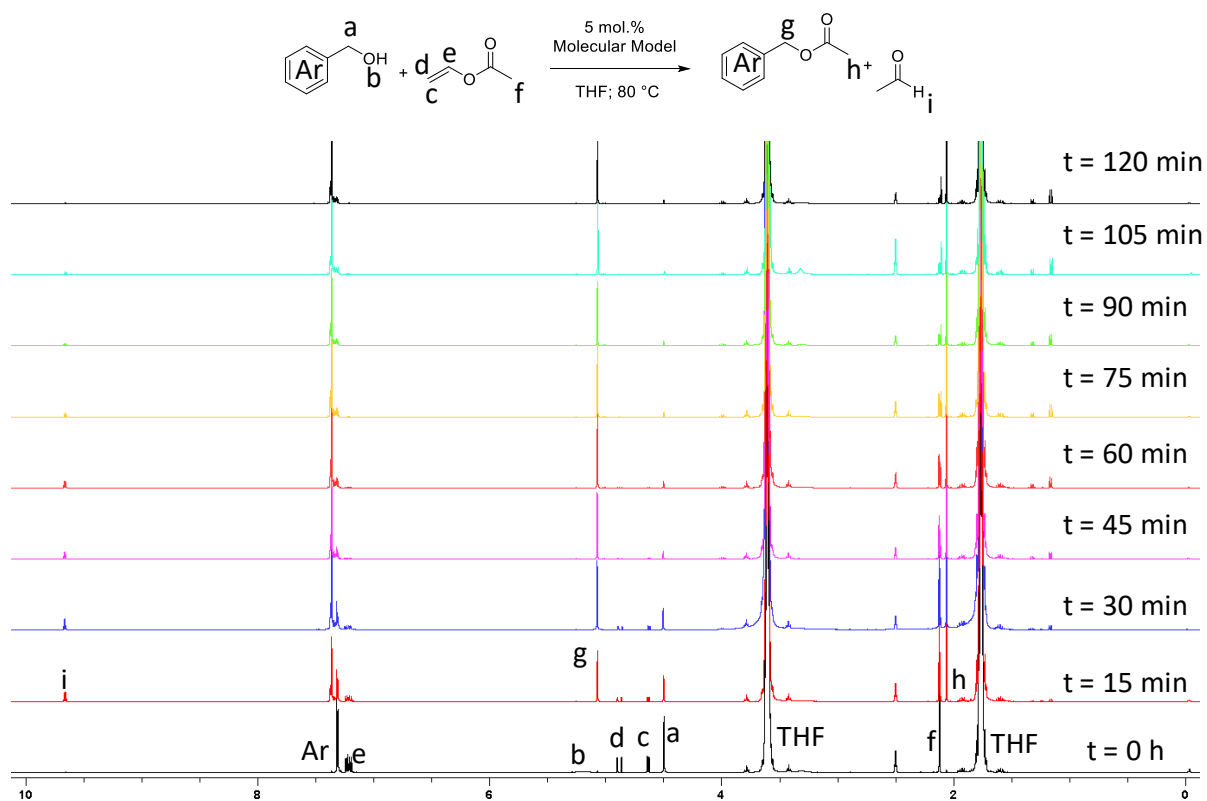


Figure S25. Reaction kinetics for run 8 (Table 1) monitored by ^1H NMR spectroscopy in $\text{DMSO}-d_6$.

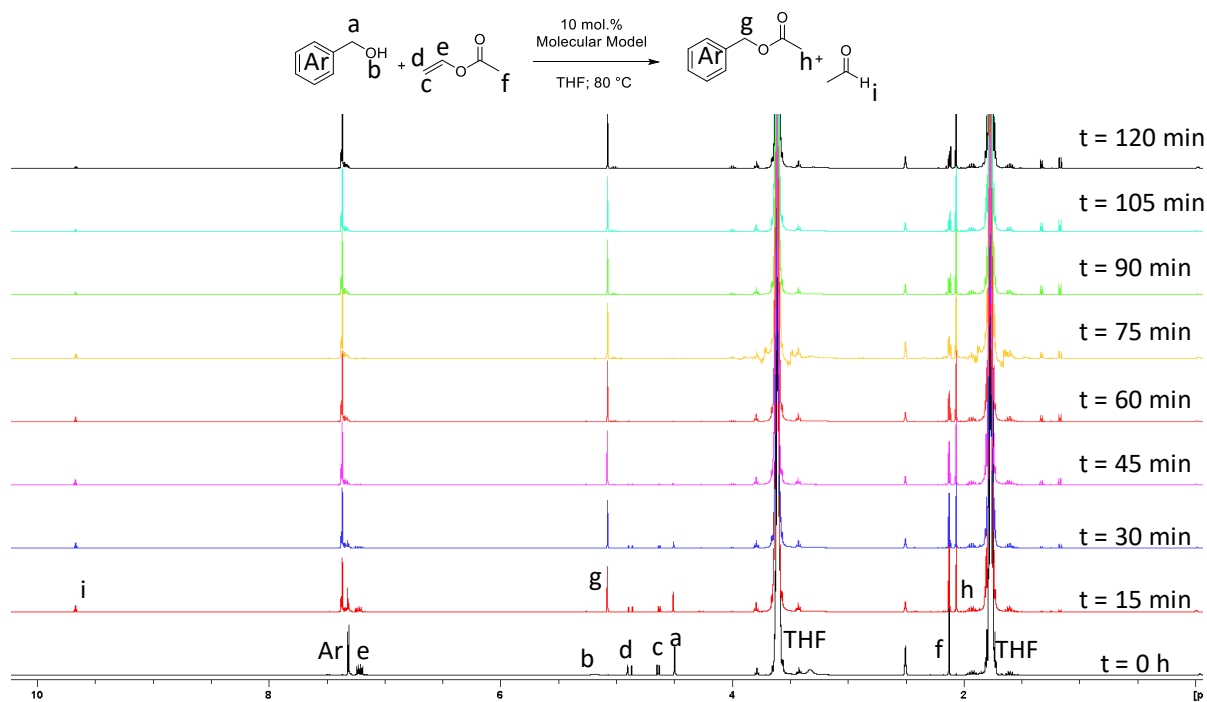


Figure S26. Reaction kinetics for run 9 (Table 1) monitored by ^1H NMR spectroscopy in $\text{DMSO}-d_6$.

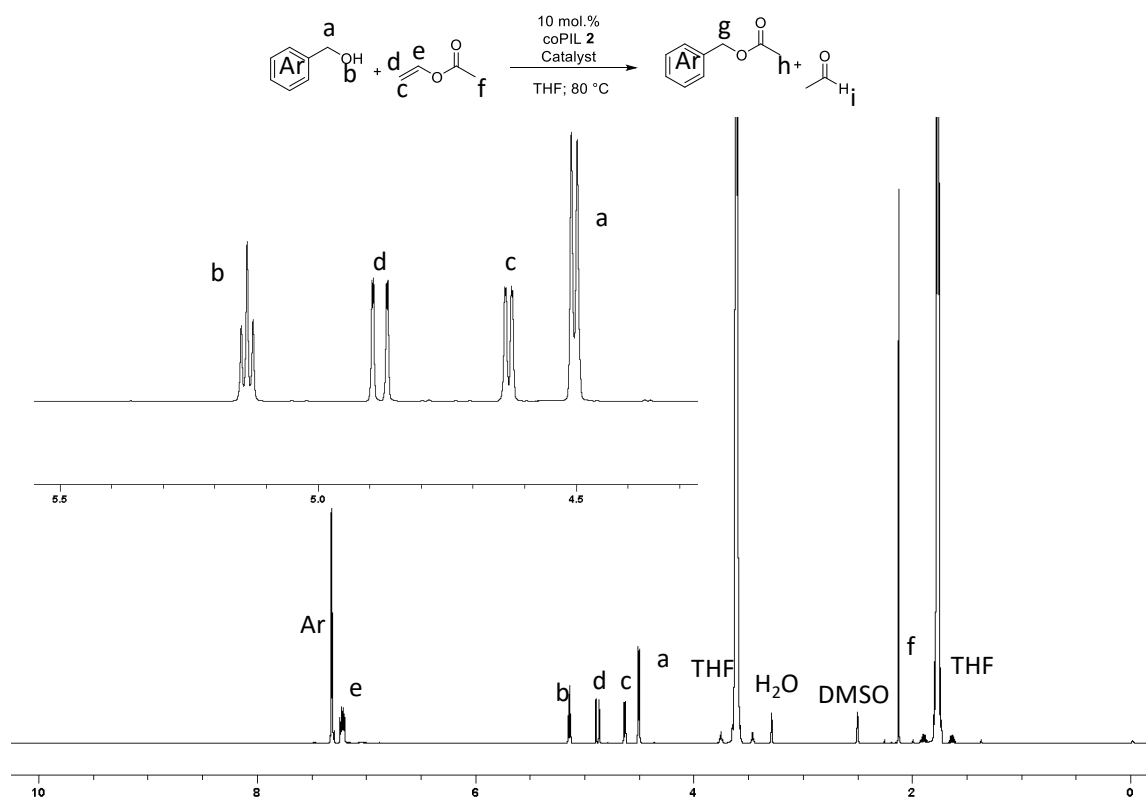


Figure S27. Reaction kinetics for run 11 (**Table 1**) monitored by ^1H NMR spectroscopy in $\text{DMSO-}d_6$

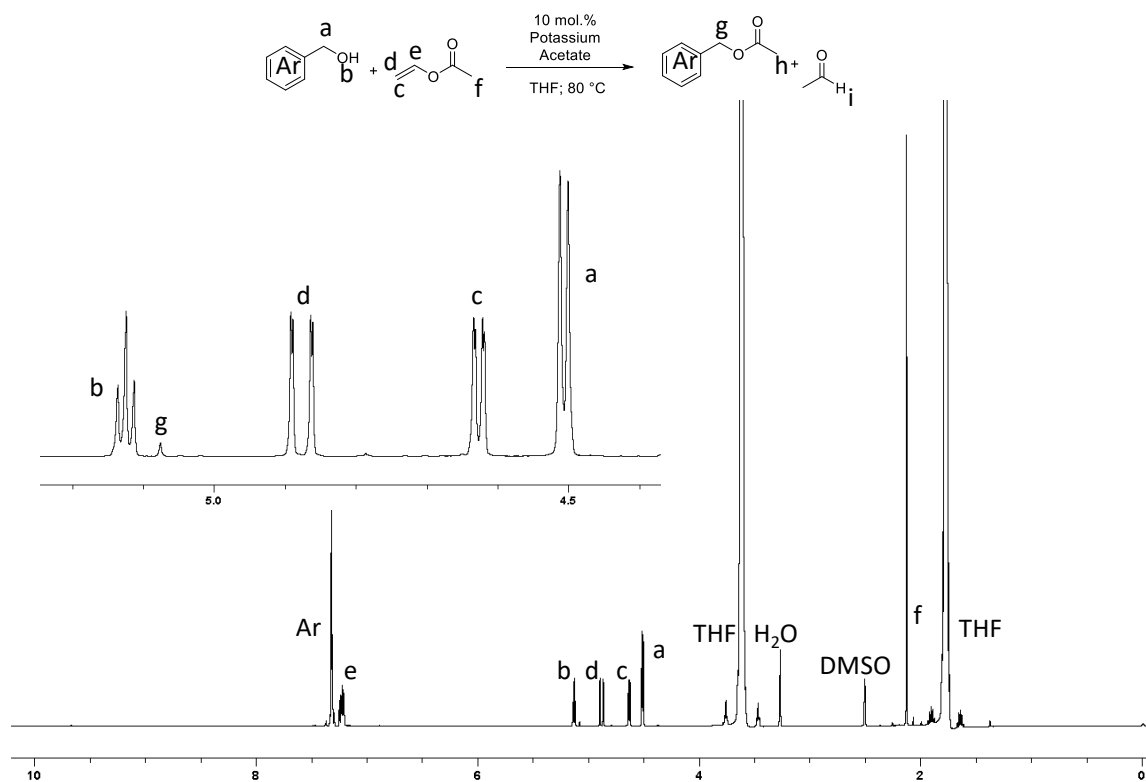


Figure S28. Reaction kinetics for run 12 (**Table 1**) monitored by ^1H NMR spectroscopy in $\text{DMSO-}d_6$.

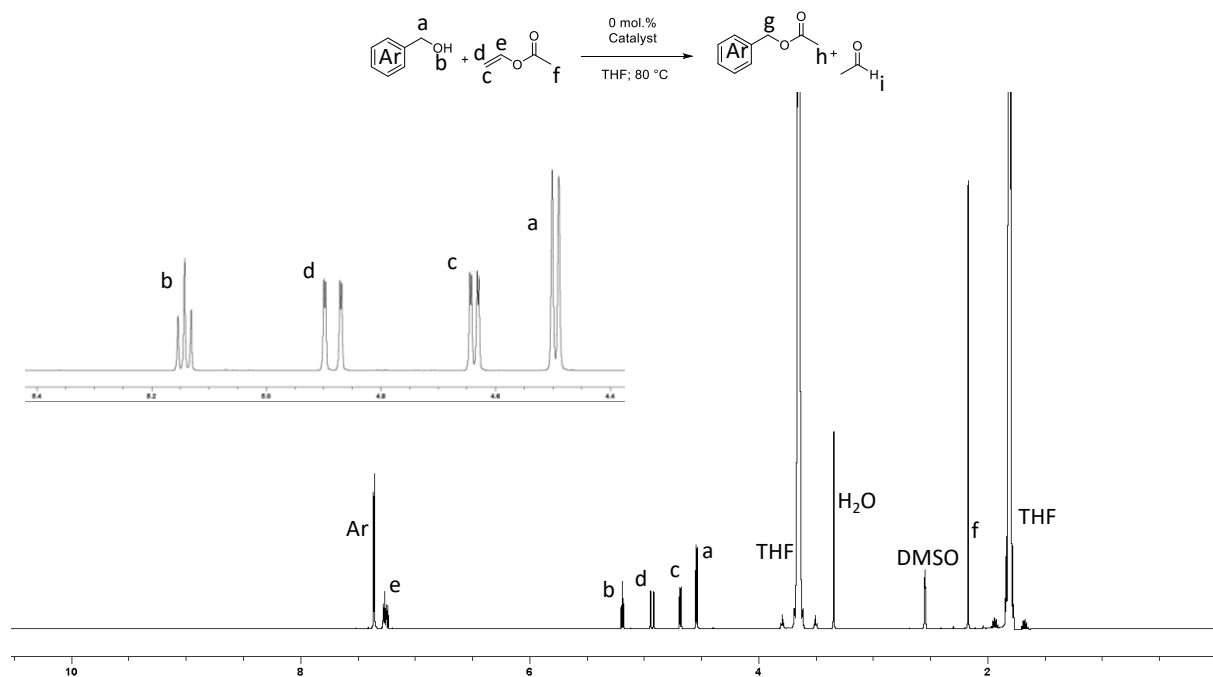


Figure S29. Reaction kinetics for run 13 (**Table 1**) monitored by ^1H NMR spectroscopy in $\text{DMSO-}d_6$.

References

- 1 S. Garmendia, R. Lambert, A.-L. Wirotius, J. Vignolle, A. P. Dove, R. K. O'Reilly and D. Taton, *Eur. Polym. J.*, 2018, **107**, 82–88.
- 2 R. Lambert, A.-L. Wirotius, S. Garmendia, P. Berto, J. Vignolle and D. Taton, *Polym. Chem.*, 2018, **9**, 3199–3204.
- 3 S. Garmendia, A. P. Dove, D. Taton and R. K. O'Reilly, *Polym. Chem.*, 2018, **9**, 5286–5294.
- 4 P. Stilbs, *Anal. Chem.*, 1981, **53**, 2135–2137.
- 5 C. S. Johnson, *Prog. Nucl. Magn. Reson. Spectrosc.*, 1999, **34**, 203–256.
- 6 L. Delaude, *Eur. J. Inorg. Chem.*, 2009, 1681–1699.
- 7 L. Delaude, X. Sauvage, A. Demonceau and J. Wouters, *Organometallics*, 2009, **28**, 4056–4064.